Experimental Evaluation of RO Membranes for Qatar Seawater Condition

Furqan Tahir and Abdelnasser Mabrouk

September 15, 2021

Article

Experimental Evaluation of RO Membranes for Qatar Seawater Condition

Furqan Tahir [1,*], and Abdelnasser Mabrouk [2]

[1] Division of Sustainable Development (DSD), College of Science & Engineering (CSE), Hamad Bin Khalifa University (HBKU), Education City, Doha 34110, Qatar; ftahir@mail.hbku.edu.qa (F.T.)
[2] Qatar Environment and Energy Research Institute (QEERI), Hamad Bin Khalifa University (HBKU), Education City, Doha 34110, Qatar; aaboukhlewa@hbku.edu.qa (A.M.)
* Correspondence: futahir@hbku.edu.qa; Tel.: +974-30074879 (F.T.)

Received: date; Accepted: date; Published: date

Abstract: The deficiency of fresh water resources in arid regions such as Gulf cooperation council (GCC) countries has compelled them to opt for desalination to fulfill their water needs. The seawater reverse osmosis (SWRO) has the lowest specific power consumption as compared to other desalination technologies. However, because of harsh seawater conditions of Qatar, thermal desalination that include multi stage flash (MSF) and multi effect desalination (MED) hold major shares in the desalination market. Recent improvements in pretreatments and membrane technology, the reverse osmosis (RO) share is growing but still more research is required to handle high salinity and unit water cost with MSF and MED technologies. In the present work, the seawater from Ras Abu Fontas, Qatar has been used to test RO membranes (Filmtec, SW30HRLE-4040). The RO test rig is comprised of four 4-inch elements in series. It is found that the permeate quality and specific power consumption improve with the feed flow rate. The salt rejection is found to be in the range of 98-99% that is below the minimum salt rejection at standard condition because of high seawater salinity. In addition, the mathematical model is developed which predicts experimental data well with the maximum error of 14.8%.

Keywords: Qatar; reverse osmosis; RO; recovery ratio; specific power consumption; salt rejection; TDS

1. Introduction

Water scarcity has become an alarming situation in many water stressed countries [1,2]. It is estimated that around 25% of world population is currently facing fresh water supply shortage and this percentage is projected to rise by 50% in 2030 [3,4]. The Gulf cooperation council (GCC) countries heavily rely on seawater desalination to meet their fresh water needs and the dependence on desalination is increasing because of the population growth and the diminishing fresh water resources [5,6]. However, desalination is energy demanding and it also affects marine life by brine rejection back to the sea, which has high salinity and temperature. Therefore, it is of utmost importance to minimize energy consumption and the associated carbon footprints by design improvements and employing energy efficient techniques for sustainable development [1,7–9].

The recovery ratio (RR) which is the percentage of desalinated water in the feed is limited by the seawater salinity. As the recovery ratio increases, the divalent cations passes the solubility limit and results in scale deposition on tube surface in multi stage flash (MSF) and multi effect desalination (MED) plants, and on reverse osmosis (RO) membranes. The salt deposition/fouling deteriorates the plant efficiency [10,11]. The enhancements in membrane materials and energy recovery devices have made seawater reverse osmosis (SWRO) energy efficient as compared to other desalination technologies [12]. The amount of ionic hardness is directly proportional to total dissolved solids

(TDS) in seawater [13]. In GCC, the Boron concentration in the seawater is very high i.e. around 7 ppm. The ionic rejection of RO membranes is in the range of 99.35% to 99.95% except Boron rejection which is limited between 70-90% [14]. Hence, two pass RO system is usually employed to keep the Boron concentration below 0.5 ppm, which is required by international regulations [15].

The main power requirement in the RO system is pumping energy which depends on seawater feed flow rate and pressure. The required power increases with the seawater salinity and minimum power requirements usually in the range of 50-55% recovery ratio [16]. In addition, high salinity increases the osmotic pressure that limits the recovery ratio. With 35% recovery ratio and 99.7% salt rejection, the permeate quality with 300-400 ppm can be achieved with a single pass RO system. However, if the permeate quality is restricted below this limit, then a two pass RO system should be opted to achieve required TDS [17,18]. The two-pass RO plant in Fujairah produces desalinated water with TDS of 75-120 ppm at an overall recovery ratio of 41%. The system consists of seawater RO in the first pass and brackish water RO in the second pass [18]. Another example of two-pass RO plant is situated in Tampa, Florida, US which employs the second pass with portion of permeate feed in first pass as the feed for second pass. This reduced the overall power consumption of the plant [19]. Some plants have been set up as a combination of thermal desalination and RO. One example if of Fujairah, UAE plant with a capacity of 454,000 m^3/day that comprises of MSF and RO units [20]. The MSF and RO operates independently but uses same intake and outfall systems. Since, MSF plant has more flexibility than RO plant for distillate production. In addition, the RO product is mixed with MSF distillate. These features have reduce the overall unit water cost [18,21]. Recently, Mabrouk et al. [22] proposed hybrid desalination plant comprised of reverse osmosis, forward osmosis and multi stage flash (RO-FO-MSF). In this configuration, the cooling reject from MSF was used as feed for the RO unit and the brine from RO was transferred as the feed for FO system. Their results showed that power consumption of RO-FO-MSF reduces by 65% when compared to MSF alone but increased by 20% with RO only. However, the unit water cost was found to be 20% and 40% lower than the RO and MSF respectively.

In Qatar, thermal desalination holds the major share in the desalination market because of steam price and harsh seawater conditions [23]. The salinity of seawater in the east side is around 45,000 ppm and for the west side it is 57,000 ppm, which is comparatively higher than the other regions [24–26]. At present, thermal desalination accounts for 76% and reverse osmosis (RO) contributes 24% in the Qatar's desalination market. The RO market is growing in the region; however, detailed analysis is required for the local conditions in terms of both power requirements and techno economics [27,28]. Present work focuses on studying RO membranes assessment for the Qatar seawater as the feed, which has a salinity of 45,000 ppm. The experiments have been performed in the RO test rig for different flow conditions to evaluate specific power consumption (SPC), salt rejection (SR) and the permeate quality. Furthermore, RO model has been established using in-house visual simulation program (VSP). The mathematical model is validated against the experimental data and is used to predict power consumption with respect to salinity variation and chemical composition across each RO membrane.

2. Experimental Setup

The commercially available reverse osmosis (RO) membranes have been characterized for Qatar seawater feed in the RO test rig, as shown in Figure 1. The Filmtec RO membranes (model: SW30HRLE-4040) used are of polyamide thin-film composite type. The characteristics of RO membranes are listed in Table 1. These membranes are designed for high saline seawater application with salt rejection rate up to 99.75%. However, salt rejection rate reported in the data sheet, is for standard test conditions and the permeate flow rate may vary by 20% per element [29]. Figure 2shows schematic for RO test rig. Four 4-inch RO elements are connected in series for which the feed flow rate is controlled by variable speed pump. The RO test rig is equipped IFM pressure gages (model: PI2692), Endress+Hauser flow meters (Proline Promag 50, DN25, model: IP67/NEMA/Type 4X), IFM temperature sensor (model: TD2807) and Endress+Hauser conductivity transmitter (model: Indumax

CLS50D). The uncertainties in these instrumentations are listed in Table 2. The test rig contains three sample points for feed, brine and permeate collection for conductivity and chemical analysis.

Figure 1. Reverse osmosis test rig

Table 1. RO membrane characteristics

Manufacturer	Filmtec
Type	Polyamide Thin-Film Composite
Model	SW30HRLE-4040
Diameter	4 inch
Maximum operating temperature	45 °C
Maximum operating pressure	83 bar
Maximum feed silt density index (SDI)	SDI 5
Active area	7.9 m²

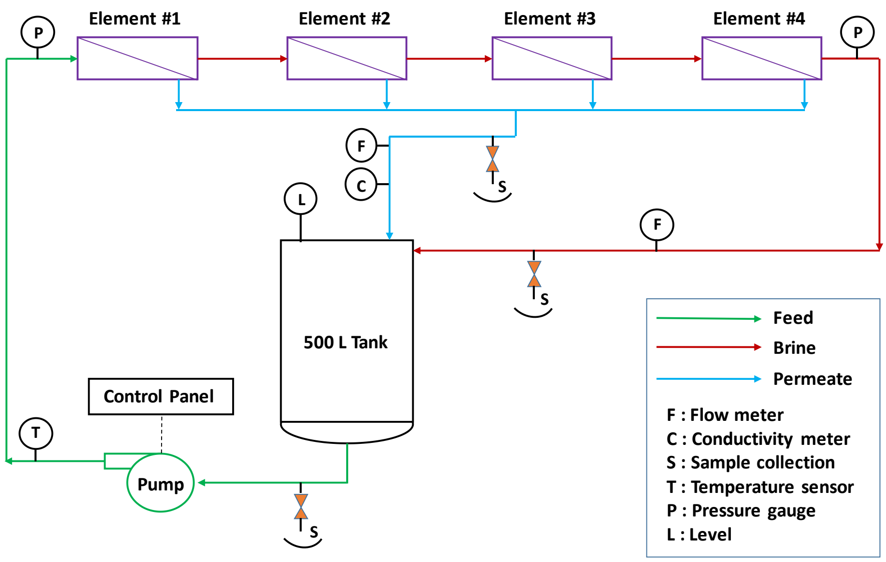

Figure 2. Process flow diagram of RO test rig

Table 2. Uncertainties in the measurements

Instrument	Uncertainty

Flow meter	± 0.5%
Pressure gauge	± 0.5%
Temperature sensor	± 0.3 °C

2.1. Seawater Collection

The seawater was collected after the pretreatment section of Ras Abu Fontas Kahramaa RO desalination plant, which is located on the east side of Qatar adjacent to Wakrah. The total dissolved solids of collected seawater was found to be 45,000 ppm.

2.2. Operating Conditions

The RO membranes have been tested for different feed flow rates F ranging from 1.6 m^3/h to 3.65 m^3/h, and the feed pressure has been varied from 35 bar to 60 bar with 5 bar interval. The total dissolved solids (TDS), specific power consumption (SPC), recovery ratio (RR) and salt rejection (SR) have been analyzed for different flow conditions.

3. Mathematical Model

The mathematical model has been developed by using in-house visual simulation program (VSP) software. The VSP software has been previously validated and implemented for thermal desalination such as multi stage flash (MSF) and multi effect desalination (MED), and membrane based desalination namely membrane distillation (MD) and reverse osmosis (RO) [22,30–33]. For RO modeling, the main equations are listed below:

$$J_w = A \cdot NDP \quad (1)$$

Where J_w is the permeate flux through RO membrane which depends on the permeability coefficient *A* and the net driving pressure *NDP*, defined by the difference in the applied pressure ΔP and osmotic pressure $\Delta\pi$.

$$NDP = (\Delta P - \Delta\pi) \quad (2)$$

The salt flux J_s through RO membrane SR is defined as:

$$J_s = B \cdot (C_{s,F} - C_{s,P}) \quad (3)$$

Where *B* is the salt permeability coefficient, $C_{s,F}$ and $C_{s,P}$ are the ionic concentrations in the feed and permeate respectively. The overall salt rejection SR of the RO membrane can be defined as:

$$SR = \frac{\left(\frac{J_w}{B}\right)}{1+\left(\frac{J_w}{B}\right)} \quad (4)$$

The specific power requirements can be evaluated from feed flow rate *F*, feed pressure ΔP, permeate flow rate *P* and pump efficiency η, which is taken as 80% in this case.

$$SPC = (100 \cdot F \cdot \Delta P)/(3.6 \cdot P \cdot \eta) \quad (5)$$

4. Results and Discussion

4.1. Experimental Results

Figure 3a shows the effect of feed flow rate on the permeate production. The feed is adjusted by increasing the pump speed to certain frequency and the pressure was set to 55 bar. It can be seen that increasing the feed flow has positive effect on the permeate production. However, the recovery ratio decreases from 27% to 21% when the feed is increased from 1.6 m^3/h to 3.65 m^3/h. The influence of feed flow rate on permeate quality is shown in Figure 3b. At low feed, the permeate quality is above 400 ppm and from 2.4-3.65 m³/h, the permeate salinity is in the range of 300-400 ppm which aligns with the studies in [17,18]. For the stringent permeate quality, two-pass RO system should be implemented. The minimum salt rejection as per RO membrane datasheet is 99.6% at standard conditions, which are 32,000 ppm of NaCl solution at 25 °C. However, with real seawater conditions and change in salinity from standard one, the salt rejection rate may vary, which is shown in Figure 4. Most of data values lies in the range of 98-99% salt rejection rate and it improves with the net driving pressure. The maximum salt rejection is 99.1% for the selected RO configuration and operating conditions.

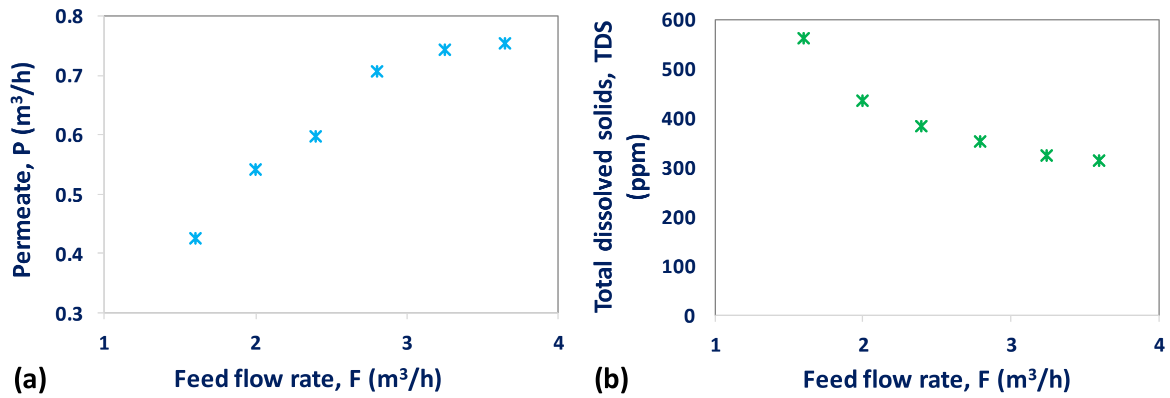

Figure 3. (a) Permeate flow rate and (b) salinity with respect to feed flow at 55 bar

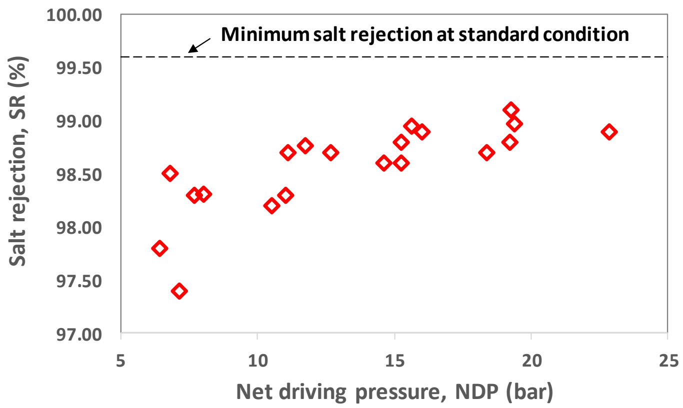

Figure 4. Salt rejection rate at different net driving pressure, *NDP*

The membrane characteristics permeability coefficient *A* and salt permeability coefficient *B* are experimentally evaluated in Figure 5a and b. Figure 5a shows effect of net driving pressure on permeate flux and the data points are fitted with linear relation. The slope of this line represents permeability coefficient *A* as per Eq. (1) and is found to be 1.36 L/m²·bar with R^2 value of 0.9208, which exhibits strong linearity between permeate flux and net driving pressure. The salt permeability coefficient *B* is estimated in Figure 5b. It is clear from experimental data that the value of *B* is not constant and varies from 0.1 to 0.3 as the net driving pressure increases. This may be due to the change in membrane characteristics such as salt diffusivity and salt partition coefficient. The specific power consumption and the recovery ratio are the key factors in assessing feasibility of desalination plant their variation with the feed flow rate is presented in Figure 6. For a fixed recovery ratio, the specific power consumption decreases as the feed flow rate increases. In addition, the specific power consumption decreases with the increasing recovery ratio. For 30% recovery ratio, the minimum specific power consumption is around 8 kWh/m³ at 3.65 m³/h. In commercial plant, energy recovery device is installed to further reduce the power consumption [19].

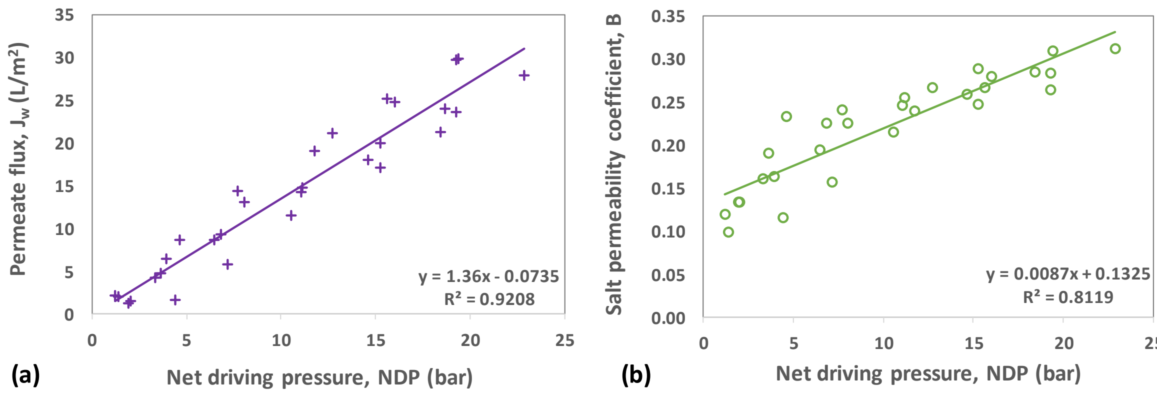

Figure 5. (a) Permeate flux, *Jw* and (b) salt permeability factor, *B* at different net driving pressure, *NDP*

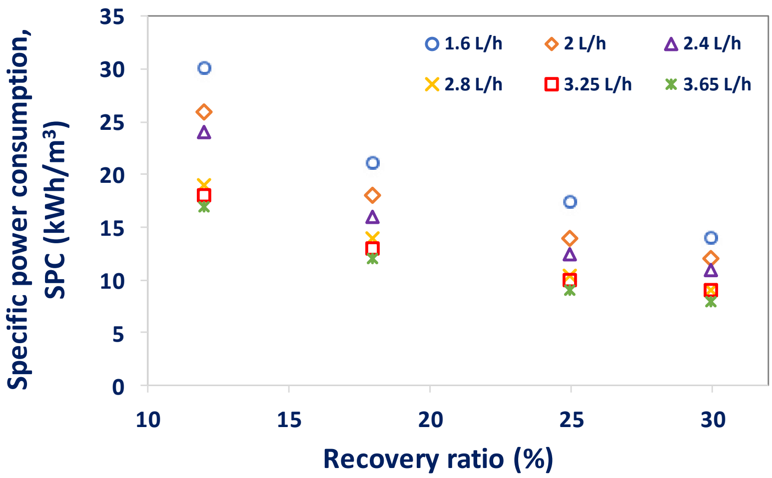

Figure 6. Specific power consumption at different recovery ratios

4.2. VSP Model Validation

The RO modeling has been carried out in VSP software, the interface of 4-elements RO system is shown in Figure 7. In order to ensure the accuracy of mathematical model, VSP results are compared with experimental data. Moreover, RO modeling has also been developed in a commercial software ROSA, which is extensively used to model RO systems. The experimental and theoretical results are compared in Figure 8. The VSP results predict experimental data well as compared to ROSA. At 1.6 m³/h, results from VSP has an error of 14.8% and for other data points, the maximum error is 8.3%. However, the results from ROSA under predicts for most of the data points and the maximum error is 18.4%.

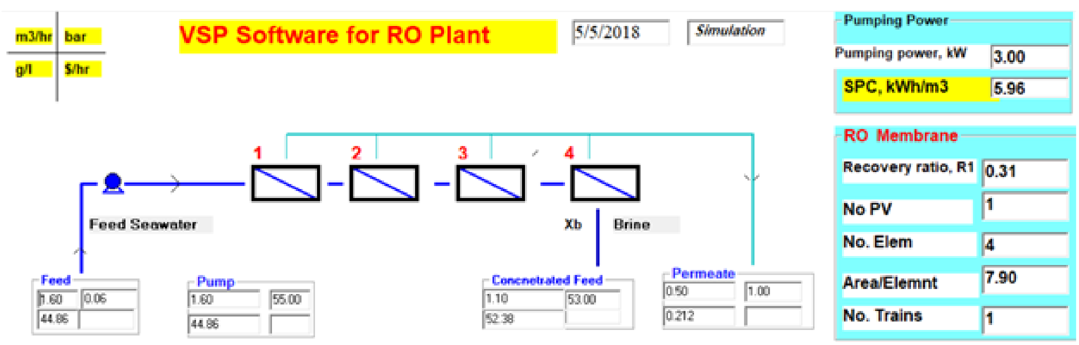

Figure 7. Four elements RO configuration in VSP software

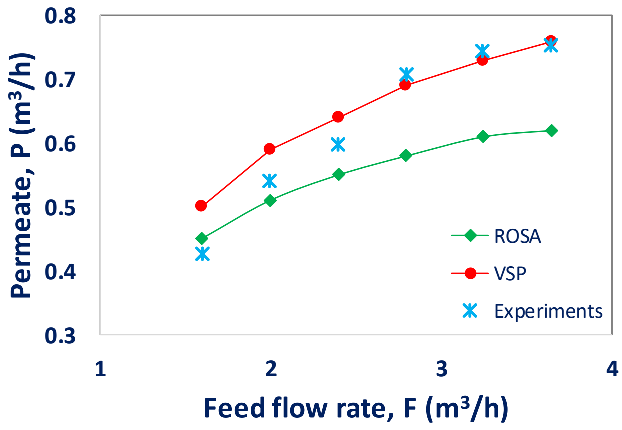

Figure 8. Comparison of experimental results with VSP and ROSA software

4.3. Chemical Analysis

Due to experimental limitations, not all data can be gathered. However, the theoretical model allows getting more insight and helps in understanding the process. The ionic distribution from VSP model across each RO element is presented in Table 3. The feed that has the salinity of 45,044 ppm has 30.6% of Na^+ and 55.2% of Cl^- ions. The Boron content in the feed for first and last element is 5.6 ppm and 8.2 ppm respectively as the brine from element issued as the feed for the next element, therefore the Boron content in the feed increases with each element. The Boron content in the permeate ranges from 0.8 to 1.1 ppm that also increases with each element. For 0.5-ppm limitation for Boron, two-pass system should be implemented. In addition, the concentration of brine after the fourth element is 65,725 ppm, which means more elements can be connected in series to increase the water output.

Table 3. Ionic concentration across each element

Ions	Element #1			Element #2		Element #3		Element #4	
	Feed	Brine	Permeate	Brine	Permeate	Brine	Permeate	Brine	Permeate
K^+	496.0	576.8	2.7	647.3	3.1	696.6	3.4	723.7	3.6
Na^+	13812.0	16061.4	74.7	18025.9	85.2	19398.9	93.6	20153.5	98.9
Mg^{+2}	1657.0	1926.9	1.8	2162.5	2.0	2327.3	2.2	2417.8	2.4
Ca^{+2}	539.0	626.8	0.6	703.4	0.7	757.0	0.7	786.5	0.8
Cl^-	24868.0	28917.9	107.6	32454.9	122.7	34927.1	134.8	36285.7	142.4
SO_4^{-2}	3472.0	4037.4	1.3	4531.3	1.5	4876.4	1.6	5066.1	1.7
HCO_3^{-1}	182.0	211.6	1.4	237.5	1.6	255.6	1.7	265.6	1.8
CO_3^{-2}	12.0	14.0	0.0	15.7	0.0	16.9	0.0	17.5	0.0
B	5.6	6.5	0.8	7.3	1.0	7.9	1.1	8.2	1.1
TDS	45043.6	52379.2	190.9	58785.8	217.8	63263.7	239.1	65724.6	252.7

5. Conclusion

In this work, seawater from Ras Abu Fontas, Qatar that has the salinity of 45,000 ppm, has been used as the feed to test commercially available seawater RO membranes (SW30HRLE-4040). The RO test rig consist of four 4-inch RO elements connected in series. The seawater feed flow rate and the pressure are varied from 1.6 to 3.65 m^3/h and 35 to 60 bar respectively. Experimental results exhibit that as the feed flow rate is increased the permeate production increases and salinity decreases. The salt rejection is found to be in the range of 98-99%, which is lower than the minimum salt rejection as per membrane specification. This due to the deviation from standard condition, the salinity of seawater is much higher than the other regions. The membrane characteristics such as water and salt permeability coefficients *A* and *B* are experimentally evaluated. The *A* and B are found to be 1.36 and 0.1-0.3 respectively. In addition, the specific power consumption decreases as as the feed flow rate and recovery ratio increases. The minimum specific power consumption is 8 kWh/m^3 at 3.65 m^3/h and 30% recovery ratio. The theoretical RO model has been developed in in-house VSP software, which predicts RO performance better than commercially available software i.e. ROSA with the maximum error of 14.8%. The permeate quality lies in the range of 300-400 ppm and the Boron content in the product varies from 0.8-1.1 ppm. It may be concluded that two-pass RO system should be chosen for Qatar seawater as the feed to keep the permeate quality below 200 ppm and the Boron content below 0.5 ppm.

Author Contributions: All authors have read and agree to the published version of the manuscript. Conceptualization, A.M.; methodology, F.T. and A.M.; software, A.M.; validation, A.M.; formal analysis, A.M.; investigation, F.T. and A.M.; resources, A.M.; data curation, F.T.; writing—original draft preparation, F.T.; writing—review and editing, A.M.; visualization, F.T.; supervision, A.M.; project administration, A.M.; funding acquisition, -.

Funding: This research received no external funding

Acknowledgments: We would like to acknowledge Qatar Environment and Energy Institute (QEERI) of Hamad Bin Khalifa University (HBKU) for the resources and support.

Conflicts of Interest: The authors declare no conflict of interest.

References

1. Tahir, F.; Baloch, A.A.B.; Ali, H. Resilience of Desalination Plants for Sustainable Water Supply in Middle East. In *Sustainability Perspectives: Science, Policy and Practice, Strategies for Sustainability*; Khaiter, P.A., Erechtchoukova, M.G., Eds.; Springer Nature Switzerland AG, 2020; pp. 303–329 ISBN 978-3-030-19550-2.
2. Tahir, F. Computational Fluid Dynamics (CFD) Analysis of Horizontal Tube Falling Film Evaporators Used in Multi Effect Desalination (MED) Plant, Hamad Bin Khalifa University, 2020.
3. Ang, W.L.; Mohammad, A.W.; Hilal, N.; Leo, C.P. A review on the applicability of integrated/hybrid membrane processes in water treatment and desalination plants. *Desalination* **2015**, *363*, 2–18.
4. Alkaisi, A.; Mossad, R.; Sharifian-Barforoush, A. A Review of the Water Desalination Systems Integrated with Renewable Energy. *Energy Procedia* **2017**, *110*, 268–274.
5. Mabrouk, A.; Abotaleb, A.; Abdelrehim, H.; Tahir, F.; Koc, M.; Abdelrashid, A.; Nasralla, A. HP MED Plants, Part II: Novel Integration MED-Absorption Vapor Compression. In Proceedings of the IDA 2017 World Congress on Water Reuse and Desalination; Sao Paulo, Brazil, 2017.
6. Tahir, F.; Mabrouk, A.; Al-Ghamdi, S.G.; Krupa, I.; Sedlacek, T.; Abdala, A.; Koc, M. Sustainability Assessment and Techno-Economic Analysis of Thermally Enhanced Polymer Tube for Multi-Effect Distillation (MED) Technology. *Polymers (Basel).* **2021**, *13*, 681.
7. Andrić, I.; Le Corre, O.; Lacarrière, B.; Ferrão, P.; Al-Ghamdi, S.G. Initial approximation of the implications for architecture due to climate change. *Adv. Build. Energy Res.* **2021**, *15*, 337–367.
8. Tahir, F.; Al-Ghamdi, S.G. Integration of MED \& HDH Desalination for an Energy Efficient Zero Liquid Discharge System. In Proceedings of the The 8th International Conference on Energy and Environment Research -- "Developing the World in 2021 with Clean and Safe Energy"; 2021; pp. 41–42.
9. Raouf, A.M.; Al-Ghamdi, S.G. Effectiveness of Project Delivery Systems in Executing Green Buildings. *J. Constr. Eng. Manag.* **2019**, *145*, 03119005.
10. Tahir, F.; Atif, M.; Antar, M.A. The Effect of Fouling on Performance and Design Aspects of Multiple-Effect Desalination Systems. In *Recent Progress in Desalination, Environmental and Marine Outfall Systems*;

2015; pp. 35–52.

11. Tahir, F.; Mabrouk, A.; Koc, M. Review on CFD analysis of horizontal falling film evaporators in multi effect desalination plants. *Desalin. Water Treat.* **2019**, *166*, 296–320.
12. *IDA Desalination Year Book 2016-2017*; Association, Global Water Intelligence and International Desalination, 2016;
13. Darwish, M. *Desalination Engineering*; Hopkinton, Ed.; 1st ed.; Balaban Desalination Publications: MA, USA, 2015; ISBN 0-86689-068-8.
14. Mabrouk, A. Hybrid thermal and membrane desalination technologies for the GCC countries. *J. Desalin. Water Purif.* **2018**, *12*, 1–3.
15. Taniguchi, M.; Fusaoka, Y.; Nishikawa, T.; Kurihara, M. Boron removal in RO seawater desalination. *Desalination* **2004**, *167*, 419–426.
16. Wilf, M.; Bartels, C. Optimization of seawater RO systems design. *Desalination* **2005**, *173*, 1–12.
17. Reverberi, F.; Gorenflo, A. Three year operational experience of a spiral-wound SWRO system with a high fouling potential feed water. *Desalination* **2007**, *203*, 100–106.
18. Sanza, M.A.; Bonnélyea, V.; Cremerb, G. Fujairah reverse osmosis plant: 2 years of operation. *Desalination* **2007**, *203*, 91–99.
19. Greenlee, L.F.; Lawler, D.F.; Freeman, B.D.; Marrot, B.; Moulin, P. Reverse osmosis desalination: Water sources, technology, and today’s challenges. *Water Res.* **2009**, *43*, 2317–2348.
20. Hamed, O.A. Overview of hybrid desalination systems — current status and future prospects. *Desalination* **2005**, *186*, 207–214.
21. Almulla, A.; Hamad, A.; Gadalla, M. Integrating hybrid systems with existing thermal desalinationplants. *Desalination* **2005**, *174*, 171–192.
22. Mabrouk, A.; Koc, M.; Abdala, A. Technoeconomic analysis of tri hybrid reverse osmosis-forward osmosis-multi stage flash desalination process. *Desalin. WATER Treat.* **2017**, *98*, 1–15.
23. Tahir, F.; Mabrouk, A.; Koc, M. Energy and exergy analysis of thermal vapor compression (TVC) and absorption vapor compression (AVC) for multi effect desalination (MED) plants. In Proceedings of the 8th Global Conference on Global Warming (GCGW), Doha, Qatar; 2019; p. 25.
24. Darwish, M.A.; Mohtar, R. Qatar water challenges. *Desalin. Water Treat.* **2013**, *51*, 75–86.
25. Dawoud, M.A.; Mulla, M.M. Al Environmental Impacts of Seawater Desalination: Arabian Gulf Case Study. *Int. J. Environ. Sustain.* **2012**, *1*, 22–37.
26. Darwish, M.; Hassabou, A.H.; Shomar, B. Using Seawater Reverse Osmosis (SWRO) desalting system for less environmental impacts in Qatar. *Desalination* **2013**, *309*, 113–124.
27. Darwish, M. Towards Energy Conservation in Qatar. *Open J. Energy Effic.* **2013**, *02*, 176–191.
28. Darwish, M.A.; Abdulrahim, H.K.; Hassan, A.S.; Sharif, A.O. Needed seawater reverse osmosis pilot plant in Qatar. *Desalin. Water Treat.* **2016**, *57*, 3793–3819.
29. FILMTEC™ FILMTEC SW30HR LE-4040 Seawater Reverse Osmosis Element Available online: https://www.lenntech.com/feedback/feedback_uk.htm?ref_title=Filmtec/Dow-Filmtec-SW30HR-LE-4040.pdf.
30. Nafey, A.S.; Fath, H.E.S.; Mabrouk, A.A. A new visual package for design and simulation of desalination processes. *Desalination* **2006**, *194*, 281–296.
31. Mabrouk, A.; Abotaleb, A.; Tahir, F.; Darwish, M.; Aini, R.; Koc, M.; Abdelrashid, A. High Performance MED Desalination Plants Part I: Novel Design MED Evaporator. In Proceedings of the IDA 2017 World Congress on Water Reuse and Desalination; Sao Paulo, Brazil, 2017.

32. Altaee, A.; Mabrouk, A.; Bourouni, K.; Palenzuela, P. Forward osmosis pretreatment of seawater to thermal desalination: High temperature FO-MSF/MED hybrid system. *Desalination* **2014**, *339*, 18–25.
33. Mabrouk, A.N.; Fath, H.E.S. Technoeconomic study of a novel integrated thermal MSF–MED desalination technology. *Desalination* **2015**, *371*, 115–125.